



Application of diffuse reflectance spectroscopy (NIR) related to soil electrical conductivity¹

Aplicação da espectroscopia de reflectância difusa (NIR) relacionada à condutividade elétrica do solo

Doris A. Meneses-Suárez², Fernando Lozano-Osorno² & Jesus H. Camacho-Tamayo^{2*}

¹ Research developed at Universidad Nacional de Colombia, Departamento de Ingeniería Civil y Agrícola, Bogotá, Colombia

² Universidad Nacional de Colombia/Facultad de Ingeniería/Departamento de Ingeniería Civil y Agrícola, Bogotá, Colombia

HIGHLIGHTS:

NIR-based spectral models allow for the identification of saline soils.

The use of geostatistics allows for the definition of sampling distances and the distribution of soil salts.

The use of NIR digital models and geostatistics allows for the creation of digital maps.

ABSTRACT: To enable the continuous evaluation and monitoring of soil salinity, diffuse reflectance spectroscopy is a promising technique because of its rapid, nondestructive nature and ability to obtain spectral signatures related to soil properties. In this research, the object was to estimate the electrical conductivity of three agricultural soils in Colombia through near-infrared (NIR) diffuse reflectance spectroscopy. A total of 377 soil samples were used to determine electrical conductivity (EC) at a ratio of 1:2 by using a netting sample system, where 0.50 × 0.50 m soil boxes were extracted to obtain undisturbed samples at two different depths. NIR spectra were obtained, and four prediction models were developed using partial least squares methodology and principal component analysis: one for each study area and one for the general area. The results revealed that the Centro Agropecuario Marengo (C.A.M.) model ($R^2 = 0.78$) and the general model ($R^2 = 0.81$) can satisfactorily estimate the EC. However, the Centro Agropecuario La Granja (C.A.G.) model ($R^2 = 0.23$) and the Centro de Investigación Carimagua, (C.I.C.) model ($R^2 = 0.15$) had low predictive ability and representativeness. A geostatistical analysis was performed to obtain digital maps. On the basis of the results, the use of diffuse reflectance spectroscopy in the NIR range is a viable alternative for estimating the EC in soils whose values are not very low (lower than 0.1 dS m⁻¹). The results indicate that diffuse reflectance spectroscopy, combined with multivariate analysis, is a reliable technique for estimating soil salinity and a nondestructive and efficient method for spatial monitoring in agricultural areas.

Key words: soil spectroscopy, electrical conductivity, near-infrared, geostatistics, salinity

RESUMO: Para permitir avaliação e monitoramento contínuos da salinidade do solo, a espectroscopia de reflectância difusa surgiu como técnica promissora devido à sua natureza rápida, não destrutiva e capacidade de capturar assinaturas espectrais relacionadas às propriedades do solo. Esta pesquisa objetivou estimar a condutividade elétrica (CE) do solo através da espectroscopia de reflectância difusa infravermelho-próximo (NIR) em três solos agrícolas na Colômbia. Um total de 377 amostras foram utilizadas para determinar condutividade elétrica, usando proporção 1:2, através de sistema de amostragem em rede, onde anéis de solo de 0,50 × 0,50 m foram extraídas para obter amostras não perturbadas em duas profundidades diferentes. Espectros NIR foram obtidos, e quatro modelos de predição foram desenvolvidos usando metodologia de mínimos quadrados parciais e análise de componentes principais: um para cada área de estudo e um geral. Os resultados mostraram que os modelos estimaram satisfatoriamente a CE para o Centro Agropecuario Marengo (C.A.M.) ($R^2 = 0,78$) e modelo geral ($R^2 = 0,81$). Entretanto, para Centro Agropecuario La Granja (C.A.G.) ($R^2 = 0,23$) e Centro de Investigación Carimagua (C.I.C.) ($R^2 = 0,15$), os modelos apresentaram baixa capacidade preditiva. Análise geostatística foi realizada para obter mapas digitais. Os resultados indicam que a espectroscopia de reflectância difusa NIR é alternativa viável para estimar CE em solos com valores não muito baixos (inferiores a 0,1 dS m⁻¹). A espectroscopia de reflectância difusa, combinada com análise multivariada, é ferramenta confiável para estimar salinidade do solo, oferecendo alternativa não destrutiva e eficiente para monitoramento espacial em áreas agrícolas.

Palavras-chave: espectroscopia do solo, condutividade elétrica, infravermelho próximo, geoestatística, salinidade



INTRODUCTION

The global population, which is projected to reach between 9 and 10.5 billion people by 2050 (Tremblay & Ainslie, 2021), is exerting increased anthropogenic pressure on soil and water systems essential for agricultural production. This demographic increase, combined with increasing food demand, has resulted in the widespread degradation of high-potential agricultural soils (Heil & Schmidhalter, 2021). Soil degradation encompasses changes in soil health that differ in terms of time, space, and function (Alqasemi et al., 2021; Wang et al., 2023), primarily because of excessive agricultural activities and inadequate resource management, which affect agricultural income, production, and food security (Camacho-Tamayo, 2013; Wang, 2023) and increase rural poverty and urban migration (Tremblay & Ainslie, 2021) through the loss of soil mass, structure, organic matter, nutrients, and other essential properties (Piccini et al., 2024).

Among the various forms of degradation, soil salinization poses the greatest risk and involves the accumulation of soluble salts. Agricultural activities are the main drivers of salinity because of excessive and inadequate irrigation with low-quality water, poor drainage, and the overuse of chemical inputs (Ordóñez & Bolívar, 2014; Qadir et al., 2014; Heil & Schmidhalter, 2021). This process alters the physicochemical balance and water retention capacity of soil, induces osmotic stress, reduces permeability, and generates nutrient imbalances that perpetuate degradation and severely reduce agricultural productivity (Bhattacharya & Bhattacharya, 2021; Gavrilescu, 2021).

Diffuse reflectance spectroscopy (DRS) is a promising solution for assessing soil salinity by examining interactions between matter and electromagnetic radiation as a function of wavelength. Each soil component has unique spectral signatures determined by absorption and reflection patterns in different regions of the electromagnetic spectrum. Most molecules absorb energy in the infrared region (4000–600 cm^{-1}), generating molecular vibrations detectable through near-infrared (NIR), mid-infrared (MIR), or far-infrared (FIR) spectroscopy (Camacho-Tamayo, 2013). These regions allow for the identification of chemical bonds, with minerals appearing in specific bands according to their composition (Camacho-Tamayo, 2013). DRS enables both quantitative and qualitative estimation of soil properties (Dematté et al., 2019) and serves as a useful technique for the indirect assessment of moisture, salt content, organic matter, and texture through molecular bond analysis. The nondestructive nature, operational speed, and cost-effectiveness make it advantageous for spatial salinity analysis compared with traditional, slower, and more expensive methods (Viscarra, 2022; Saad et al., 2024).

In Colombia, salinization presents particular challenges because of climatic factors (low rainfall, high evaporation, and salt-rich parent materials) and anthropogenic factors related to inadequate irrigation and drainage management. A National Study on Soil Degradation by Salinization (IDEAM, 2019) revealed that 46.6% of the Colombian territory is susceptible to salinization, with 0.7% having very high susceptibility, making

salinity research essential for conservation, management, and territorial planning strategies. Colombia has implemented policies such as the National Ecological Restoration Plan, which requires ongoing support for research and monitoring to ensure sustainable production and food security (Lal et al., 2021; MINAMBIENTE, 2021; Bhaduri et al., 2022). In Colombia, applications include mineralogical characterization in the Cauca River Valley (Obando & Carbonell, 2010), property determination in Puerto Gaitán Oxisols with soil moisture estimation (Carranza Díaz et al., 2023), organic carbon assessment (Fernández-Martínez et al., 2022), total carbon estimation (Fernández-Martínez et al., 2023), and spectral analysis in alluvial zones (Rincón et al., 2023). The objective of this study was to evaluate the hypothesis that NIR diffuse reflectance spectroscopy can accurately predict soil electrical conductivity (EC) in three Colombian agricultural soils, whose prediction accuracies differ according to salinity levels and physicochemical properties.

MATERIAL AND METHODS

Three specific locations were selected for soil sampling to evaluate a range of edaphoclimatic conditions (Table 1). Samples were obtained in 2018, in March (Centro Agropecuario Marengo, C.A.M.), June (Centro Agropecuario La Granja, C.A.G.) and September (Centro de Investigación Carimagua, C.I.C.). This approach facilitated the comparative analysis of electrical conductivity (EC) in areas with distinct environmental characteristics. Table 1 presents the principal information for each of the analyzed soils.

First, the “Centro Agropecuario Marengo” is located in a cold, dry environmental climate with an average annual precipitation of 1,124 mm and exhibits a bimodal pattern with a period of 128 mm from March to June and a period of 156 mm from October to November. The mean annual temperature is 12.7 °C, with a maximum of 19.6 °C and a minimum of 5.3 °C. The air relative humidity ranged from 75 to 90%. The relief of the area consists of a floodplain with terrace-like landforms, with slopes ranging from 1 to 3%, and depressions with slopes < 1% (Ordóñez & Bolívar, 2014). The soils in the C.A.M. area

Table 1. Information on the analyzed soils

Soil order	Place	Location	Mean climatic conditions
Oxisol	Centro de Investigación Carimagua (C.I.C.)	4° 34' 01.6" N 71° 19' 58.0" W Average altitude: 170 m.a.s.l.	Temperature: 31 °C Wind velocity: 18 km h ⁻¹ Air relative humidity: 59%
	Puerto Gaitán (Meta)		
Alfisol	Centro Agropecuario La Granja (C.A.G.)	4° 10' 17.6" N 74° 55' 44.4" W Average altitude: 312 m.a.s.l.	Temperature: 25 °C Wind velocity: 18 km h ⁻¹ Air relative humidity: 59%
	Espinal (Tolima)		
Inceptisol	Centro Agropecuario Marengo (C.A.M.)	4° 42' 52.0" N 74° 12' 60.0" W Average altitude: 2516 m.a.s.l.	Temperature: 13 °C Wind velocity: 8 km h ⁻¹ Air relative humidity: 68%
	Mosquera (Cundinamarca)		

m.a.s.l.: meters above sea level. The soil order is based on the USDA classification for soil taxonomy (Soil Survey Staff, 2022)

are developed from fine or medium alluvial deposits, with a predominance of Inceptisols, mostly with fine textures and clayey, clay loam, and silty clay loam textural classes.

The “Centro Agropecuario La Granja” is located in a warm, dry climate of tropical dry forest, where precipitation exhibits a bimodal pattern, with precipitation being 160 mm in April and 150 mm in October. The average annual temperature is 27 °C. The slope of the area is slightly flat, with slopes < 7%. The predominant soils in the area are Alfisols with a sandy loam texture (IGAC, 1970; Ortega-Monsalve et al., 2023).

The “Centro de Investigación Carimagua” presents flat to lightly undulating slopes ranging from 2 to 5%. The soils in the center are very deep, well-drained soils developed from clayey alluvial sediments, where highly aggregated and strongly acidic Oxisols predominate (pH < 5) (Camacho-Tamayo, 2013).

For the present study, a total of 377 samples were used: 154 samples from Marengo (Figure 1A), 147 samples from El Espinal (Figure 1B), and 76 samples from Carimagua (Figure 1C). The samples from Carimagua and El Espinal were previously extracted and were available in the Soil Laboratory of the Department of Civil and Agricultural Engineering of the Universidad Nacional de Colombia.

According to Cortés-D et al. (2013), the C.A.M. soil profile reveals a strong agricultural potential because of its favorable chemical and physical properties. The pH values, which ranged from 5.3 to 5.9, were within the slightly acidic range optimal for most crops, whereas the relatively high organic carbon content (0.21–2.8%) indicated good soil fertility and structure. The sandy loam to clay loam texture provides adequate water retention and drainage balance. Most notably, the moderate to high electrical conductivity values (0.9–2.4 dS m⁻¹) suggest sufficient nutrient availability, and reasonable porosity levels (48.1–62.5%) ensure proper aeration and root development.

According to Ortega-Monsalve et al. (2023), the C.A.G. soil profile has excellent agricultural characteristics because of its consistent fine texture throughout the profile, which improves its water and nutrient retention abilities. A moderate organic carbon content (0.39–0.99%) provides an adequate soil fertility basis for crop production. The bulk density values, which ranged from 1.71 to 1.93 g cm⁻³, remained within acceptable limits for root development and water movement. The uniform fine texture across all horizons (0–0.25 m depth) ensures consistent growing conditions and facilitates effective nutrient distribution, making this soil suitable for crops that benefit from high water retention and nutrient-holding capacity.

The C.I.C. soil profile, as reported by IGAC (1970), exhibits excellent agricultural suitability, particularly because of its optimal pH range (5.03–5.38) that favors nutrient uptake for most agricultural crops. Low electrical conductivity values (0.05–0.25 dS m⁻¹) indicate minimal salinity stress, creating favorable conditions for crop establishment and growth. The sandy loam to clay loam texture provides an ideal balance between drainage and water retention capacity. Additionally, the moderate porosity values (45.9–48.1%) and appropriate bulk density (2.7–2.8 g cm⁻³) suggest a good soil structure that supports root penetration and water infiltration.

Each of the samples had different depths depending on the type of crop planted at each site. Soil sampling was conducted

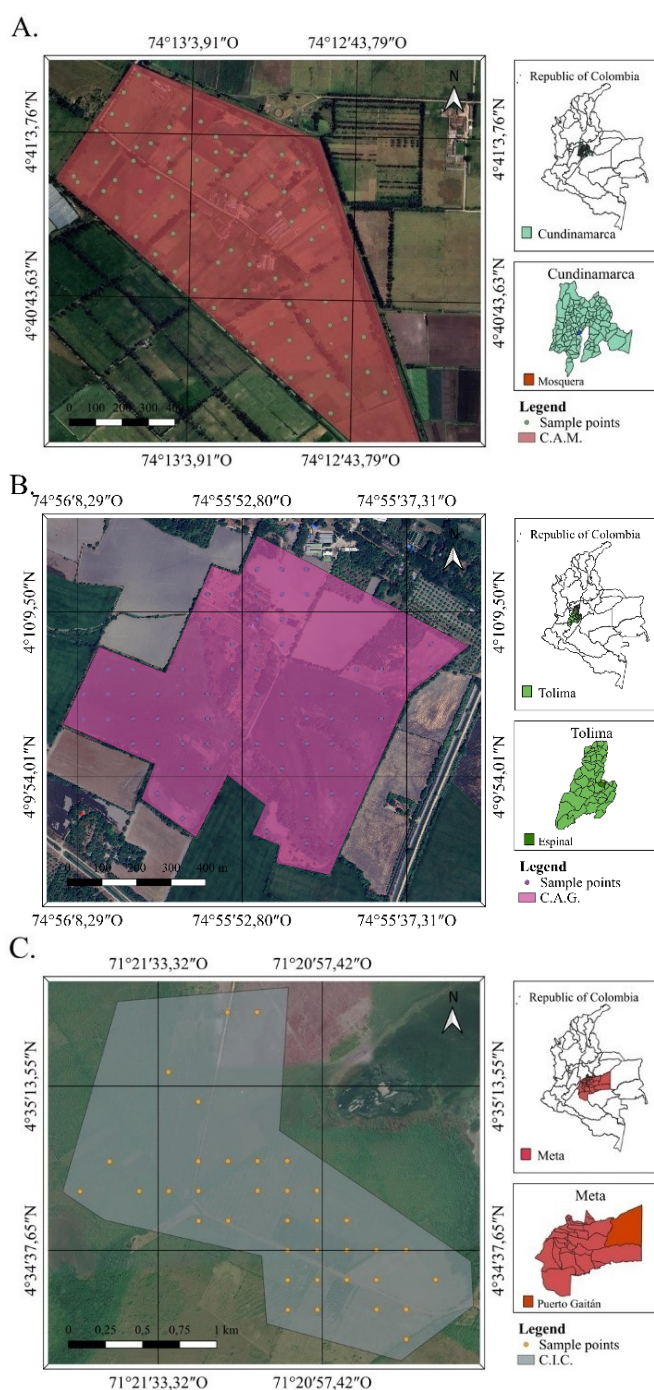


Figure 1. Location of the 77 sample points in Centro Agropecuario Marengo (A), 74 sample points in Centro de Investigación Carimagua (B), and 40 sample points in Centro Agropecuario La Granja (C)

in three agricultural research centers using methods adapted to the characteristics of each area. At C.A.M., 77 sampling points were used at depths of 0.10 and 0.35 m across an area of approximately 90 ha, on the basis of the soil information from Ordóñez & Bolívar (2014). At C.A.G., a fixed grid was applied over 50 ha, encompassing 9 plots, with 74 sampling points at depths of 0.10 and 0.25 m, according to Ortega-Monsalve et al. (2023). At C.I.G., a directed network was established over an area of 5100 ha, with 40 sampling points at depths of 0.10 and 0.30 m, according to Fernández-Martínez et al. (2023). In all the cases, representativeness of the A and B horizons was ensured by excavating soil pits of 0.50 × 0.50 × 0.50 m.

After the selection and collection of samples were completed, the samples were taken to the Soil and Geomatics Laboratories of the Faculty of Engineering and Agricultural Sciences. The C.A.M. samples were dried at 35 °C for 72 hours to achieve a near-zero moisture content. The C.I.C. samples were dried at 35 °C for 48 hours, whereas the C.A.G. samples were left at ambient temperature until they reached equilibrium moisture. All the samples were subsequently ground and sieved to 2 mm (No. 10 mesh) to remove detrital material and homogenize the particle size.

To determine the electrical conductivity for the saturation point (EC_{se}) and pH, a pH meter (C5020, Consort, Turnhout, Belgium) was used. A soil-to-water ratio of 1:2 was used to determine the values of the corresponding EC_{se} and pH.

A descriptive statistical analysis was subsequently performed on the obtained EC_{se} and pH data. This analysis included calculating the mean, maximum, minimum, standard deviation, coefficient of variance (CV), and range. Additionally, the Grubbs test ($p \leq 0.05$) was applied to identify and remove any outliers. These analyses were performed using the statistical software GraphPad Prism 9. Random samples were chosen, with 75% allocated to the calibration set and 25% allocated to the validation set. Efforts were made to ensure that the range of values in the validation dataset remained within the limits defined by the calibration dataset, because the latter serves as the empirical basis on which the model generates its predictions. If the validation data exceed this range, the model may lack the necessary variability to adequately represent the validation samples, affecting the quality and validity of the predictive model.

To obtain spectra in the NIR region (1000–2500 nm), an FT-NIR spectrometer (NIRFlex N500, Büchi Labortechnik, Switzerland) with a resolution of 8 cm⁻¹ was used. Prior to spectral acquisition, the soil samples were ground to pass through a 2-mm sieve and air-dried at room temperature for 48 hours to standardize the moisture content. Approximately 3–5 g of each sample was placed in standard sample cups and leveled to ensure a uniform surface presentation. For each sample, one reading was obtained with 32 scans to improve the spectral quality while maintaining a reasonable analysis time, with the spectral data recorded as log(1/R) values where R represents the reflectance.

The model calibration and selection process were based on the spectral profile in which the peaks were more clearly accentuated, facilitating the reading and interpretation of the spectrum and improving the visibility of relevant information. The decision was supported by different statistical indicators, based on root mean square error (RMSE) and coefficient of determination (R^2) were compared to determine which yielded better results. Preprocessing techniques such as the standard normal variate (SNV) and Savitzky–Golay derivative were subsequently applied to correct dispersion and noise in the data. Calibration was performed using partial least squares regression (PLSR), and cross-validation was employed to evaluate the calibration model results, in addition to external validation. In terms of PLSR, the factors represent the components required to reconstruct the original dataset and explain the relationships between the predictor variables and the response variable. These factors condense

relevant information by decomposing the model into latent components that increase its explanatory power on the basis of statistical indicators such as the RMSE and R^2 . However, when a calibration model requires many factors, it may indicate overfitting: the model overexplains the data and produces overly optimistic results that do not reflect its true predictive ability. Therefore, a model with fewer factors and strong statistical performance is preferable to increase robustness.

The loading weight method enables the selection of significant variables, such as characteristic wavelengths, for a prediction model. These variables are derived from the calibration model obtained through PLSR. With respect to each latent variable, which correspond to a specific wavelength, the number of selected wavelengths must match the number of latent variables (Rodríguez-Pérez et al., 2021).

PLSR uses a prediction matrix X (the spectrum matrix) and a response variable vector Y (the soil property) to construct a prediction model in which an orthogonal basis of successive latent variables is constructed, which are ordered according to their relevance and increase the covariance between the predictor X and the variable Y (Viscarra et al., 2006). This relationship is written as follows (Eq. 1):

$$Y = \beta_0 + \beta_{\lambda_1} X_{\lambda_1} + \dots + \beta_{\lambda_n} X_{\lambda_n} \quad (1)$$

where:

Y - represents the variable to be predicted (dS m⁻¹);

β_0 - denotes the y-intercept;

$\beta_{\lambda_1} \dots \beta_{\lambda_n}$ - indicate the regression coefficients for each wavelength; and,

$X_{\lambda_1} \dots X_{\lambda_n}$ - reflectance or absorbance values for each wavelength.

The following statistical parameters were used: coefficient of determination (R^2), root mean square error (RMSE), standard error (SE), and residual prediction deviation (RPD) for the calibration and cross-validation sets of the model. In terms of external validation, the coefficient of determination (R^2) and standard error (SEP) were calculated for the validation set. To detect outliers, a Hotelling's T-square distribution was employed, and loading weights were used to identify significant wavelength regions. These analyses were conducted using the multivariate statistical software Unscrambler X 10.4 (CAMO Software AS, Oslo, Norway).

A geostatistical analysis was performed to assess the spatial dependence of electrical conductivity. Experimental semivariograms were constructed for the measured and predicted data at each of the sampling depths. These semivariograms allow us to analyze the relationship between the data obtained for a variable at different points within a specific area in terms of direction and distance, assuming that the values of the property being analyzed are more similar at short distances than those located at greater distances. Matheron (1963) defined the function of the experimental semivariogram as shown in Eq. 2.

$$\gamma(h) = \frac{1}{2N(h)} \sum_i^{N(h)} [Z(x) - Z(x+h)]^2 \quad (2)$$

where:

$Z(x)$ - is the value of the variable z at location x (m);

$Z(x + h)$ - is the value of the variable z separated from the previous point by a distance h (m); and,

$N(h)$ - is the number of pairs separated by h .

There are theoretical models that fit the experimental semivariogram. In this study, spherical, exponential, and Gaussian-bounded models, as defined by Webster & Oliver (2007), were considered (Eqs. 3 to 5).

- Spherical:

$$\gamma(h) = \begin{cases} C_0 + C_1 \left[1.5 \times \left(\frac{h}{a} \right) - 0.5 \times \left(\frac{h}{a} \right)^3 \right]; & h \leq a \\ C_0 + C_1; & h > a \end{cases} \quad (3)$$

- Exponential:

$$\gamma(h) = \begin{cases} C_0 + C_1 \left[1 - e^{-\frac{3h}{a}} \right]; & h \leq a \\ C_0 + C_1; & h > a \end{cases} \quad (4)$$

- Gaussian:

$$\gamma(h) = C_0 + C_1 \left[1 - e^{-\frac{h^2}{a^2}} \right] \quad (5)$$

where:

$\gamma(h)$ - is Gaussian model (dS m^{-1});

Nugget (C_0) - indicates variability or discontinuity between samples (dS m^{-1});

Sill ($C_0 + C_1$) - indicates the value at which the semivariogram stabilizes and stops changing (dS m^{-1}); and,

Range (a) - represents the distance (h) at which spatial correlation occurs.

The degree of spatial dependence (DSD) was subsequently determined as proposed and classified by Cambardella et al. (1994), as shown in Eq. 6:

$$\text{DSD}(\%) = 100 \times \frac{C_1}{C_0 + C_1} \quad (6)$$

where:

Weak if $\text{DSD} \leq 25\%$;

Moderate if $25\% < \text{DSD} \leq 75\%$; and,

Strong if $\text{DSD} > 75\%$.

With respect to the selection of theoretical semivariogram models, the coefficient of determination (R^2) was used. After these models were chosen, digital maps of spatial distribution were created using ordinary kriging interpolation, considering cross-validation. These procedures were conducted using GS+ v. 10 software (Gamma Design Software, LLC, Plainwell, MI).

RESULTS AND DISCUSSION

After the calibration and validation sets were selected, a descriptive statistical analysis was performed for each of the soils used. The following results were obtained (Table 2). With respect to model prediction, both the absorbance and reflectance responses were evaluated as initial pretreatment options. In terms of the C.A.M. model, a better response was obtained with absorption, whereas in terms of the C.A.G. and C.I.C. models and the global model that combined the three soils, a better response was obtained with reflectance (Tables 2 and 3).

The statistical results (Table 2) revealed significant differences in the performance of the prediction models according to the evaluated zone. With respect to the C.A.M. and global models, determination coefficients (R^2) exceeding 0.75 in calibration and satisfactory values in external validation (0.68–0.70) indicate an acceptable level of prediction, albeit with signs of overfitting that could be mitigated by expanding the number and range of samples. These models additionally exhibited RPD values between 1.7 and 1.9, which supports their applicability for quantitative estimations of electrical conductivity. In contrast, the C.A.G. and C.I.C. models had $R^2 < 0.25$ and RPD values approaching 1, indicating that they were classified as poor and lacking reliable predictive ability, which is reinforced by the high prediction errors obtained. NIR spectroscopy constitutes a promising technique for predicting electrical conductivity in soils with moderate to high salinity levels or through integrated models; however, its efficacy is limited in low-salinity soils where variability and representativeness restrict precision.

To remove irrelevant information, noise, deviation, and dispersion caused by particle diameter from spectral responses, in terms of the C.A.M., C.A.G., and global models, smoothing was performed using a second derivative of Savitsky-Golay (with a polynomial of order 2) and SNV normalization. In the case of the C.I.C. model, in addition to applying the same pretreatments, the first derivative of Savitsky-Golay and an MSC were used, but the best results were only the spectrum without pretreatment for reflectance, and the electrical conductivity was measured in dS m^{-1} .

For each of the prediction models, a PLSR was performed, and the β values obtained for the construction of a prediction model in the form of Eqs. 7–10 are shown in Table 3.

Table 2. Results of the descriptive statistical analysis in terms of electrical conductivity for the calibration and validation sets (dS m^{-1})

Model	Set	Maximum	Minimum	Mean	SD	CV
C.A.M.	Cal.	5.57	0.040	0.820	0.95	1.16
	Val.	5.29	0.148	0.972	1.12	1.15
C.A.G.	Cal.	0.45	0.002	0.101	0.06	0.64
	Val.	0.30	0.033	0.103	0.06	0.62
C.I.C.	Cal.	0.37	0.014	0.089	105.95	1.19
	Val.	0.27	0.015	0.056	66.94	1.19
Global	Cal.	5.57	0.002	0.401	0.73	1.81
	Val.	5.29	0.017	0.422	0.78	1.84

Note: Cal. - calibration set and Val. - Validation set; Set - Sample set; SD - Standard deviation; CV - Coefficient of variation

Table 3. Equations for obtaining β values for the proposed models

Model	Equation
C.A.M.	$CE = \beta - 5.43 \times 10^{-5} \beta_{1000} \dots - 0.02979 \beta_{2418.16}$ (7)
C.A.G.	$CE = \beta - 0.2170 \beta_{1003.21} \dots + 0.1737 \beta_{2480.16}$ (8)
C.I.C.	$CE = \beta - 40.90 \beta_{1000} \dots + 32.13 \beta_{2500}$ (9)
Global	$CE = \beta + 0.00025 \beta_{1000} \dots - 0.0075 \beta_{2480.16}$ (10)

To evaluate the validity of the model, cross-validation, followed by external validation, was performed. The statistical parameters obtained for the calibration and validation of each electrical conductivity prediction model are listed below (Table 4).

On the basis of the criteria of Rodríguez-Pérez et al. (2021), the C.A.M. and global models, which are satisfactory ($0.50 \leq R^2 \leq 0.75$) but could be improved either with a larger number of samples or ranges of the measured values, achieved the best predictions, whereas the C.A.G. and C.I.C. models performed poorly ($R^2 < 0.50$) and had minimal predictive ability and representativeness.

In terms of the C.A.M. and global models, the results differed from those obtained by Farifteh et al. (2018), who obtained a precision of 20.8%, which indicates a low potential for identifying types of salts in the near-infrared region and shortwave infrared region (VNIR-SWIR) (400 - 2500 nm), and in the predictive models, they obtained $0.51 \leq R^2$ of cross-validation ($CV \leq 0.87$) for different types of salt. Tsolis & Barouchas (2023) reported an R^2 in the middle infrared (MIR) of 0.79 for soil carbon, and McBride (2022) reported an R^2 of 0.80 for various soil chemical properties, whereas the results obtained with the C.A.G. and the C.I.C. models were lower than those reported by Viscarra et al. (2022), who reported the best R^2 of 0.38 in the MIR.

The behavior of the prediction precision suggested by Minasny et al. (2009) and Rodríguez-Pérez et al. (2021) indicates a reasonable prediction with $RPD > 1.5$ of the Marengo Agricultural Center and the global model, and for the C.A.G. and the C.I.C. models there is no reliable prediction, and it was not recommended to use this calibration models to estimating electrical conductivity in these soils. A regression analysis was performed with the measured and estimated values, in which low R^2 values were obtained for the C.A.G. and the C.I.C. models, indicating that the estimated values provide some information but with high variance, confirming the low predictive ability of these models (Figures 2B and C). On the other hand, with respect to the C.A.M. and global models, the variability between the data was greater for the measured and estimated data (Figures 2A and D).

The previous differences between the models and those discussed in the literature can be attributed to the spectral

response of the soils analyzed, as well as the methods and measurement conditions in the laboratory. In accordance with the methods of Ordóñez & Bolívar (2014), the soil at Marengo was classified as saline because of the high levels of soluble salts and electrical conductivity exceeding established thresholds. This condition limits plant development and represents a permanent restriction on land use capacity. According to Farifteh et al. (2018), an increase in salinity produces changes in reflectance and decreases the albedo of the spectrum obtained from the soil. Tsolis & Barouchas (2023) attributed the poor prediction of models to inadequate normal distribution or low variability. These authors also indicated that it is better to calibrate models for samples from the same dataset, which in this study would be constructing a model for each soil type or for those associated with specific conditions and environments (Chamara et al., 2022).

In addition, the low potential to identify types of salts and electrical conductivity is attributed to the finding that most absorption features occur near the water absorption bands at approximately 1400 and 1900 nm (Chamara et al., 2022) and can mask the salts, whose bands are usually reported between approximately 1440 and 1933 nm and are consistent with those reported for water (Farifteh et al., 2018). The electrical conductivity of the soil is not related to the matrix or the solid constituents of the soil and is affected by the region, landscape, land use, climatic factors and electrolyte concentration; therefore, it is not accurately predicted (Farifteh et al., 2018; Viscarra et al., 2022; Wang, 2023).

The most representative wavelengths for each model were obtained from the loading weights (Figure 3). With respect to the C.A.M. model (Figure 3A), they are 1410-1417, 1870-1960, and 2180-2220 nm; with respect to the C.A.G. model (Figure 3B), they are approximately 1410, 1880-1900, and 2200-2226 nm; with respect to the C.I.C. model (Figure 3C), they are approximately 1410, 1890, and 2180-2210 nm; and with respect to the global model, they are approximately 1386-1415, 1860-1960, and 2190-2210 nm (Figure 3D). These intervals represent the wavelengths that capture the most relevant information from the reflectance process for ECse.

After the representative wavelengths for each zone have been identified, it is important to determine what information these peaks reveal. Electrical conductivity is not a direct property of the soil and can be associated with other soil properties, such as pH, and relies on the amount and type of salt present in the soil. Farifteh et al. (2018) reported information about the spectral behavior of salt-affected soils to explore the relationship between the response and the concentration of salt present in the soil and observed characteristic vibrations of anions for salts such as epsomite at wavelengths near 1300 and 2400 nm; bischofite at wavelengths near 1000, 1200, 1400, and 1900 nm; halite and sylvite at wavelengths near 1440 and

Table 4. Statistical parameters obtained from the prediction models

Site model	Calibration				Cross-validation			External validation	
	R^2	RMSE	SEC	RMSE	R^2	SECV	RPD	R^2	SEV
C.A.M.	0.780	0.444	0.446	0.549	0.677	0.551	1.723	0.701	0.607
C.A.G.	0.235	0.056	0.057	0.061	0.134	0.061	1.056	0.181	0.058
C.I.C.*	0.159	9.623	9.715	10.402	0.055	10.494	1.010	N/A	9.783
Global	0.813	0.313	0.314	0.381	0.727	0.382	1.912	0.683	0.438

R^2 - Coefficient of determination; RMSE - Root mean square error; SEC - Calibration standard error; SECV - Crossed validation standard error; RPD - Prediction residual deviation; SEV - External validation standard error. * The units of EC were measured in $dS m^{-1}$. N/A - Not applicable - The model did not provide representative values

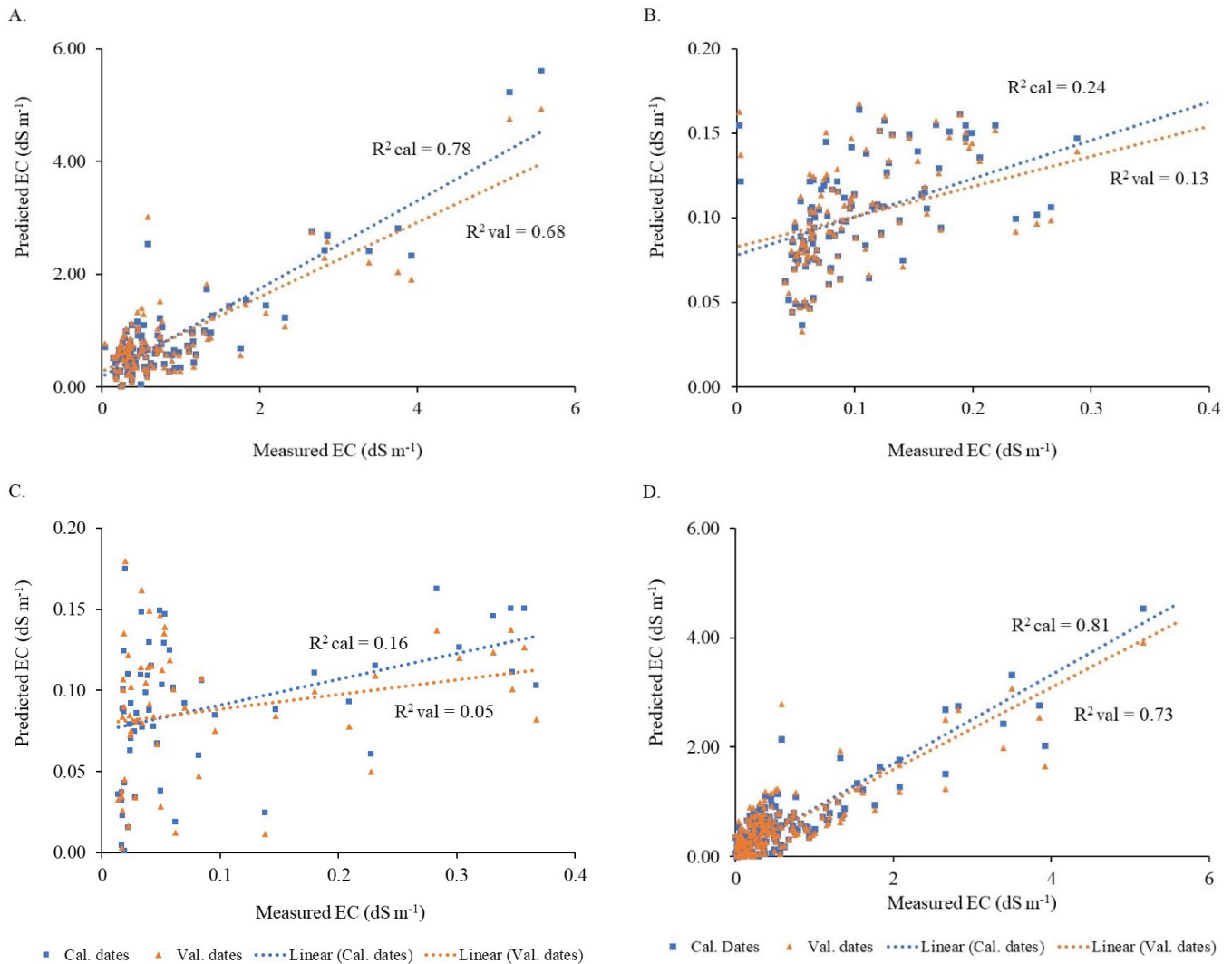


Figure 2. Cross-validation of measured electrical conductivity of saturation extract (EC_{se}) versus predicted EC_{se} for Centro Agropecuario Marengo (A), Centro Agropecuario La Granja (B), Centro de Investigación Carimagua (C), and the global model (D)

1933 nm; thenardite at wavelengths near 1410 and 1929 nm; and arcanite at wavelengths near 1430, 1932, and 2080 nm, and in the wavelength near 1631 nm, it is present in severely saline soils (Farifteh et al., 2018).

Thus, on the basis of Farifteh et al. (2018) and the representative wavelengths identified, minerals such as bischofite, thenardite, and arcanite could be present in the Centro Agropecuario Marengo; thenardite, bischofite, and arcanite could be present in the Centro Agropecuario La Granja; and thenardite could be present in the Centro de Investigación Carimagua. However, laboratory studies are necessary to confirm the type of salt present.

Principal component analysis was performed to determine whether it was possible to identify groups by depth, location, or soil type in the dataset (Figure 4). With respect to the C.A.M. model (Figure 4A), the first two components represent 74% of the explained variance, where the first principal component discriminates 59% of the total samples, whereas the second principal component discriminates 15% of the total samples. Notably, there is a difference in the depths given by PC2. The data from depths of 0–0.35 m are separated from those from depths of 0–0.10 m, which can also be explained by the negative part of this principal component.

Principal component analysis (PCA) is a statistical technique used to reduce the dimensionality of a dataset by grouping variability into new vectors referred to as principal components (Abdel-Fattah et al., 2021). The first component (PC1) reflects the largest portion of explained variability, clustering samples that exhibit similar patterns. The second component (PC2) accounts for the variability that is not explained by PC1 but reflects internal similarities within another group of samples, etc., with subsequent components. This transformation facilitates the visualization of natural groupings within the dataset. For example, if distinct differences are observed between PC1 and PC2 based on soil depth, the results from one depth are significantly different from those from another depth, allowing for objective differentiation.

With respect to the C.A.G. model (Figure 4B), the first two components represent 90% of the explained variance, where the first principal component discriminates 60% of the total samples, whereas the second principal component discriminates 30% of the total samples. Compared to the C.A.M. model, a greater spectral difference can be observed. In this case, the groups are represented by PC1. The data from depths of 0–0.25 m are separated from those from depths

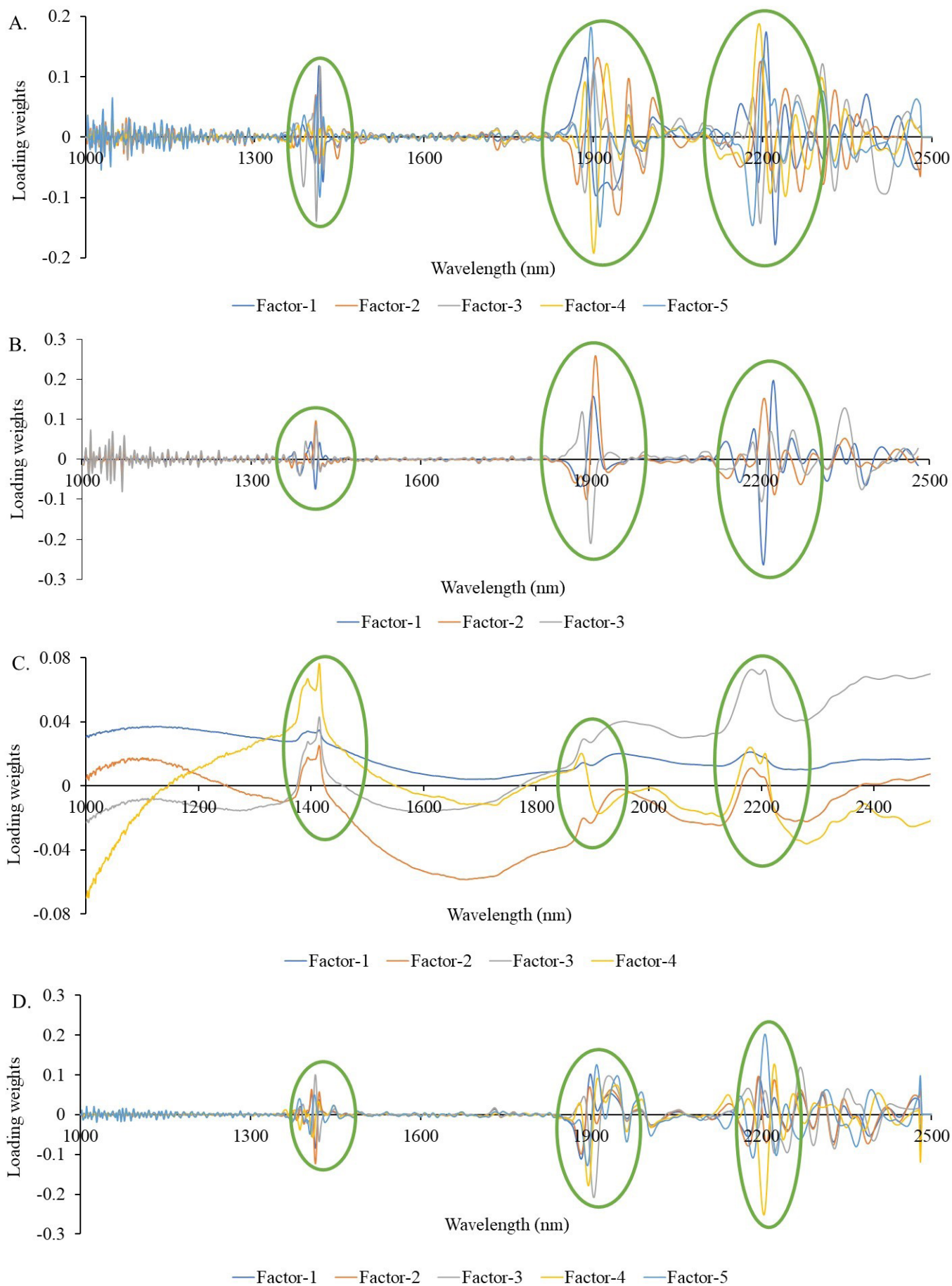


Figure 3. Representative wavelengths for the Centro Agropecuario Marengo (A), Centro Agropecuario La Granja (B), Centro de Investigación Carimagua (C), and (D) global models

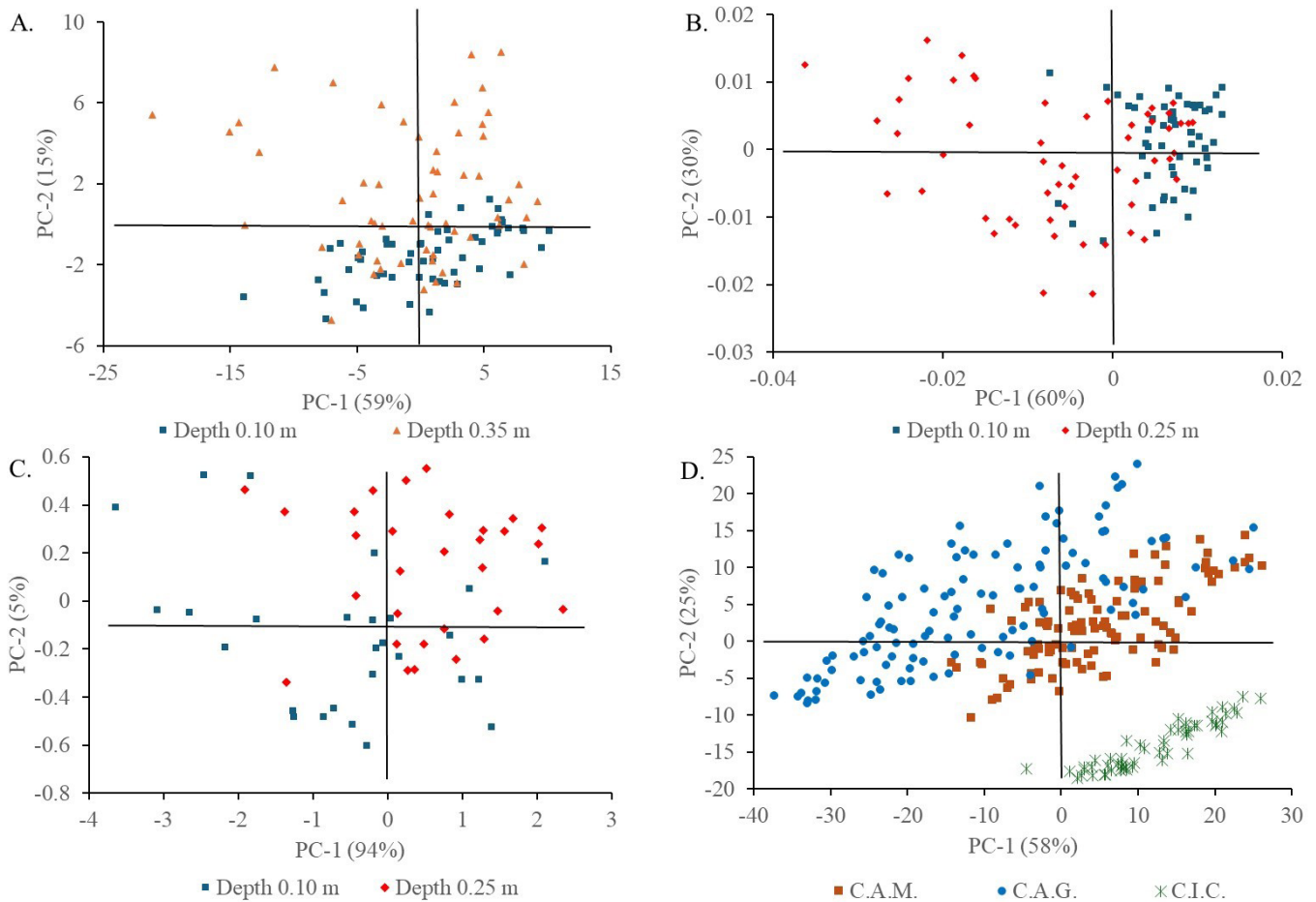


Figure 4. Score plot for principal component analysis for the Centro Agropecuario Marengo (A), Centro Agropecuario La Granja (B), Centro de Investigación Carimagua (C), and (D) global models

of 0–0.10 m, which can also be explained by the negative component of this principal component.

With respect to the C.I.C. model (Figure 4C), the first two components represent 99% of the explained variance, where the first principal component discriminates 94% of the total samples, whereas the second principal component discriminates 5% of the total samples. In terms of this soil, although the variance is almost completely explained, there is no distinct difference in the electrical conductivity values according to depth.

With respect to the global model (Figure 4D), the first two components represent 83% of the explained variance, where the first principal component discriminates 58% of the total samples, whereas the second principal component discriminates 25% of the total samples. The difference is attributed to the location, where the difference in the soil of the C.I.C. model was greater than those of the other two models and is explained by the negative component of PC2, whereas the soil of the C.A.G. and C.A.M. is explained mainly by the positive component of PC2.

The geostatistical analysis for electrical conductivity was conducted using theoretical semivariogram analysis (Table 5), employing the results from the laboratory and those estimated by the prediction model. In terms of the measured data at depths of 0.10 to 0.30 m from the C.I.C. model, no representative semivariogram model was obtained because of the pepita effect.

With respect to the semivariogram fitting models, the same models were not obtained for the measured and predicted data for the same study area and the two depths analyzed. The models were only consistent for the predicted values in the Centro Agropecuario La Granja, whereas in the Centro Agropecuario Marengo, the measured and predicted values showed the same model in terms of depth. At depths of 0.10 to 0.35 m, the results are consistent with those observed by Cortés-D et al. (2013).

Good semivariogram models with $R^2 > 0.90$ were obtained, along with models with satisfactory estimations with $R^2 > 0.60$. Additionally, the degree of spatial dependence (DSD) obtained for most models was strong, with the exception of the Centro Agropecuario La Granja, which had a moderate DSD. In terms of the Centro Agropecuario Marengo, the DSD coincides with the findings reported by Cortés-D et al. (2013), where a strong DSD was obtained. The ranges obtained for each of the study areas increased as the soil depth increased, indicating a lower spatial variability in electrical conductivity (Ortega-Monsalve et al., 2023).

On the basis of the representative models, interpolation surfaces were generated using the ordinary Kriging method with the measured data and those predicted by the prediction model for each depth used in this study, in which the distribution and trend of soil salinity can be observed by Mukhamediev et al. (2023) and the quality of the prediction models. Although the maps are similar, there are intrinsic uncertainties in the

Table 5. Theoretical semivariogram parameters for electrical conductivity

Study zone	Depth (m)	Model	Co	C ₁ +Co	Range, a	R ²	DSD	CVC
Laboratory results								
C.A.M.	0 – 0.10	Gaussian	1.00E-03	0.9310	184	0.65	0.99	0.81
	0 – 0.35	Spherical	0.1160	0.6290	734	0.74	0.82	0.82
C.I.C.	0 – 0.10	Spherical	490	22080	1403	0.97	0.98	0.68
	0 – 0.30	Nugget effect		9355				
C.A.G.	0 – 0.10	Spherical	8.97E-04	2.75E-03	397	0.93	0.67	0.90
	0 – 0.25	Exponential	4.10E-04	9.64E-03	1317	0.91	0.96	0.66
Models estimation results								
C.A.M.	0 – 0.10	Gaussian	0.043	0.751	246	0.69	0.94	1.23
	0 – 0.30	Spherical	0.073	0.427	601	0.72	0.83	1.01
C.I.C.	0.10	Gaussian	390	1612	620	0.95	0.76	0.70
	0 – 0.30	Nugget effect		1691				
C.A.G.	0 – 0.10	Spherical	9.40E-05	1.15E-03	574	0.99	0.92	0.99
	0 – 0.25	Spherical	4.34E-04	1.09E-03	891	0.81	0.60	1.03

Co - Nugget; C₁+Co - Sill; DSD - Degree of spatial dependence; and CVC - Cross-validation coefficient for the C.A.G. - Centro Agropecuario La Granja, C.I.C. - Centro de Investigación Carimagua, and C.A.M. - Centro Agropecuario Marengo models

area, and the ranges of electrical conductivity differ between the measured and predicted values.

In terms of the C.A.M. model (Figure 5), the highest values of electrical conductivity are concentrated in lots 1 to 4, with values ranging from 1 to 5.5 dS m⁻¹ for both depths of 0–10 cm and 10–35 cm, which can be attributed to the use of fertilizers in permanent and semipermanent crops and that this area has salinity problems. Therefore, intervening and managing these areas properly is necessary to stop the cumulative progress of salts (Mukhamediev et al., 2023), because the values obtained indicate a much higher concentration of salts in these areas than in the other two study areas.

In addition, the digital maps obtained from the predicted and measured values are similar in relation to the depth. The predictive ability of the model is reflected in the maps; at depths of 0 to 10 cm, it tends to overestimate the value of the electrical conductivity, whereas at depths of 10 to 35 cm, the values are more similar to the measured values, indicating a good predictive ability of the model.

With respect to the C.A.G. model (Figure 6), there are noticeable differences between the measured and predicted values. At a depth of 10 - 30 cm, the value estimated by the model exhibits a spatial behavior similar to the previous depth, with a slight decrease in electrical conductivity along the soil

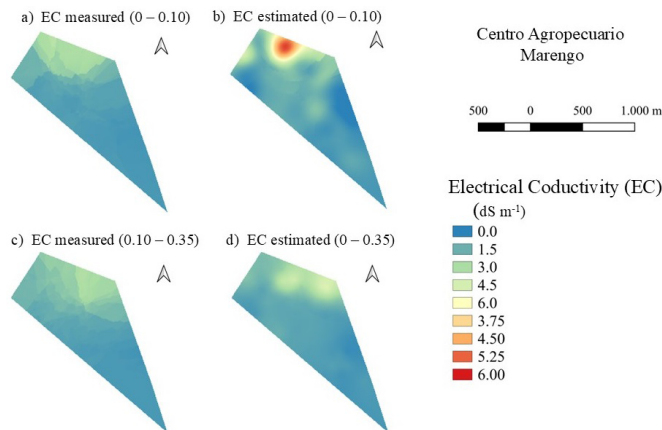


Figure 5. Digital maps of electrical conductivity (EC) for the Centro Agropecuario Marengo. obtained from measured data (A and C) and estimated data (B and D) for the two sampling depths analyzed

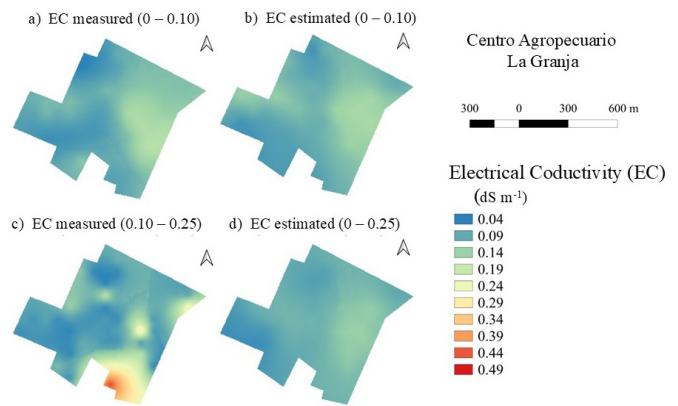


Figure 6. Digital maps of electrical conductivity (EC) for the Centro Agropecuario La Granja (C.A.G.) obtained from measured data (A and C) and estimated data (B and D) for the two sampling depths analyzed

profile. However, compared with the measured values, the model tends to underestimate them for this area. There is a higher concentration of salts in the southern part of the study site, which can be attributed to the use of fertilizers in permanent and semipermanent crops. However, these values are not high enough to classify the soil as saline. Notably, if adequate and constant monitoring is not available, the soil will gradually degrade.

In terms of the C.I.C. model (Figure 7), there is a high level of variability in the results of the interpolation of the measured and predicted data (0-10 cm depth), in addition to the lack

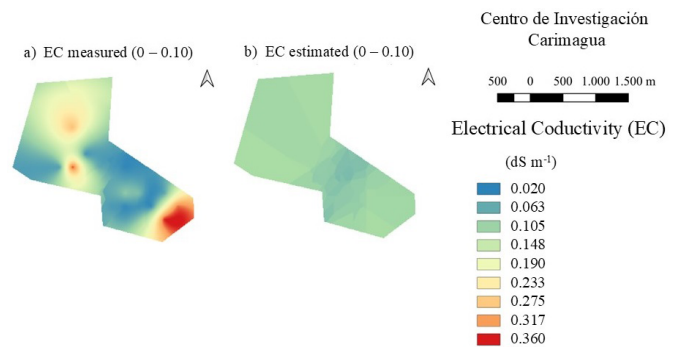


Figure 7. Digital maps of electrical conductivity (EC) for the Centro de Investigación Carimagua obtained from measured data (A) and estimated data (B) at depths of 0 - 10 cm

of good correlation between the digital maps. This finding can be attributed to the low predictive ability of the model ($R^2 = 0.16$) and the small number of samples, which affects the spatial analysis and, in turn, the correspondence between maps (Camacho-Tamayo et al., 2013).

CONCLUSIONS

1. Diffuse reflectance spectroscopy in the near-infrared (NIR) region was found to be an effective technique for predicting soil electrical conductivity in Colombian agricultural contexts, particularly in soils with salinity levels above 0.5 dS m^{-1} . The models developed for the Centro Agropecuario Marengo yielded results comparable to those of conventional methods, confirming the applicability of NIR spectroscopy as a rapid monitoring technique.

2. The high prediction errors and low performance of the models developed for the Centro Agropecuario La Granja and the Centro de Investigación Carimagua suggest that the technique has limitations in non-saline soils, highlighting the need to expand the sample range and consider environmental factors.

3. The models from Centro Agropecuario Marengo and the global dataset showed greater accuracy when more samples and higher EC ranges were included. These models also enabled the discrimination of samples by depth and soil type, as indicated by principal component analysis (PCA), confirming the potential of the technique for multivariate studies, soil zoning, and territorial planning.

4. Digital maps generated through geostatistical analysis allow for precise visualization of the horizontal spatial distribution of soil salinity within a given region, facilitating monitoring, identification of critical zones, and management of affected or at-risk areas.

Contribution of authors: D. A. Meneses-Suarez supported soil sample collection and laboratory work, data acquisition, and manuscript writing. F. Lozano-Osorno supported the methodological development and data processing. J. H. Camacho-Tamayo supervised the research and supported sample processing, data analysis, and manuscript writing.

Data availability statement: The authors declare that there are no data underlying the text.

Conflict of interest: The authors declare that they have no conflicts of interest.

Financing statement: The authors have not received research grants from any agency or organization.

LITERATURE CITED

- Abdel-Fattah, M. K.; Mohamed, E. S.; Wagdi, E. M.; Shahin, S. A.; Aldosari, A. A.; Lasaponara, R.; Alnaimy, M. A. Quantitative evaluation of soil quality using Principal Component Analysis: The case study of El-Fayoum depression Egypt. *Sustainability*, v.13, e1824, 2021. <https://doi.org/10.3390/su13041824>
- Alqasemi, A. S.; Ibrahim, M.; Fadhil Al-Quraishi, A. M.; Saibi, H.; Al-Fugara, A. K.; Kaplan, G. Detection and modeling of soil salinity variations in arid lands using remote sensing data. *Open Geosciences*, v.13, p.443-453, 2021. <https://doi.org/10.1515/geo-2020-0244>
- Bhaduri, D.; Sihi, D.; Bhowmik, A.; Verma, B. C.; Munda, S.; Dari, B. A review on effective soil health bio-indicators for ecosystem restoration and sustainability. *Frontiers in Microbiology*, v.13, e938481, 2022. <https://doi.org/10.3389/fmicb.2022.938481>
- Bhattacharya, A. Effect of soil water deficit on growth and development of plants: a review. In: Bhattacharya, A. (ed.). *Soil water deficit and physiological issues in plants*. Singapore: Springer, 2021, Cap.5, p.393-488. https://doi.org/10.1007/978-981-33-6276-5_5
- Camacho-Tamayo, J. H. Uso de la reflectancia difusa -NIR en la determinación de características físicas y químicas de un Oxisol. Carimagua -Meta. 1.ed. Bogotá: Universidad Nacional de Colombia, 2013. 149p.
- Cambardella, C. A.; Moorman, T. B.; Novak, J. M.; Parkin, T. B.; Karlen, D. L.; Turco, R. F.; Konopka, A. E. Field-scale variability of soil properties in central Iowa soils. *Soil Science Society of America Journal*, v.58, p.1501-1511, 1994. <https://doi.org/10.2136/sssaj1994.03615995005800050033x>
- Carranza-Díaz, A. K.; Camacho-Tamayo, J. H.; Rubiano-Sanabria, Y. Validación de un modelo para la estimación del contenido de agua del suelo mediante espectroscopía en el infrarrojo cercano. *Revista U.D.C.A Actualidad & Divulgación Científica*, v.26, e2329, 2023. <https://doi.org/10.31910/rudca.v26.n1.2023.2329>
- Chamara, N.; Islam, M. D.; Bai, G. F.; Shi, Y.; Ge, Y. Ag-IoT for crop and environment monitoring: Past, present, and future. *Agricultural Systems*, v.203, e103497, 2022. <https://doi.org/10.1016/j.agsy.2022.103497>
- Cortés-D.; D. L.; Pérez-B., J. H.; Camacho-Tamayo, J. H. Relación espacial entre la conductividad eléctrica y algunas propiedades químicas del suelo. *Revista UDCA Actualidad & Divulgación Científica*, v.16, p.401-408, 2013. <https://doi.org/10.31910/rudca.v16.n2.2013.912>
- Demattê, J. A. M.; Dotto, A. C.; Bedin, L. G.; Sayão, V. M.; Souza, A. B. Soil analytical quality control by traditional and spectroscopy techniques: Constructing the future of a hybrid laboratory for low environmental impact. *Geoderma*, v.337, p.111-121, 2019. <https://doi.org/10.1016/j.geoderma.2018.09.010>
- Farifteh, J.; van der Meer, F.; van der Meijde, M.; Atzberger, C. Spectral characteristics of salt-affected soils: A laboratory experiment. *Geoderma*, v.145, p.196-206, 2018. <https://doi.org/10.1016/j.geoderma.2008.03.011>
- Fernández-Martínez, F.; Camacho-Tamayo, J.H.; Rubiano-Sanabria, Y. Estimating texture and organic carbon of an Oxisol by near infrared spectroscopy. *Revista Ciência Agronômica*, v. 53, e20218167, 2022. <https://doi.org/10.5935/1806-6690.20220020>
- Fernández-Martínez, F.; Rubiano-Sanabria, Y.; Camacho-Tamayo, J. H. Near-infrared spectroscopy: Assessment of soil organic carbon stock in a Colombian Oxisol. *Ingeniería e Investigación*, v.43, e1648, 2023. <https://doi.org/10.15446/ing.investig.99102>
- Gavrilescu, M. Water, soil, and plants interactions in a threatened environment. *Water*, v.13, e2746, 2021. <https://doi.org/10.3390/w13192746>
- Heil, K.; Schmidhalter, U. An evaluation of different NIR-spectral pre-treatments to derive the soil parameters C and N of a humus-clay-rich soil. *Sensors*, v.21, e1423, 2021. <https://doi.org/10.3390/s21041423>
- IDEAM - Instituto de Hidrología, Meteorología y Estudios Ambientales. Protocolo para la identificación y evaluación de la degradación de suelos por salinización en Colombia. 2017. Available on: <<https://bit.ly/3MtYBTm>>. Accessed on: April 2025.

- IGAC - Instituto Geográfico Agustín Codazzi. Estudios semidetallados y general de suelos de los municipios de la Dorada, Caldas, Honda y Armero Tolima. Bogotá, 1970. Available on: <https://descubridor.banrepcultural.org/discovery/fulldisplay/alma991004089779707486/57BDLRDC_INST:57BDLRDC_INST>. Accessed on: April 2025.
- Lal, R.; Bouma, J.; Brevik, E.; Dawson, L.; Field, D. J.; Glaser, B.; Hatano, R.; Hartemink, A. E.; Kosaki, T.; Lascelles, B.; Monger, C.; Muggler, C.; Ndzana, G. M.; Norra, S.; Pan, X.; Paradelo, R.; Reyes-Sánchez, L. B.; Sandén, T.; Singh, B. R.; Spiegel, H.; Yanai, J.; Zhang, J. Soils and sustainable development goals of the United Nations: An international union of soil sciences perspective. *Geoderma Regional*, v.25, e00398, 2021. <https://doi.org/10.1016/j.geodrs.2021.e00398>
- Matheron, G. Principles of geostatistics. *Economic Geology*, v.58, p.1246-1266, 1963. <https://doi.org/10.2113/gsecongeo.58.8.1246>
- McBride, M. B. Estimating soil chemical properties by diffuse reflectance spectroscopy: Promise versus reality. *European Journal of Soil Science*, v.73, e13192, 2022. <https://doi.org/10.1111/ejss.13192>
- MINAMBIENTE - Ministerio de Ambiente y Desarrollo Sostenible. La conservación y protección del suelo es otro de los logros ambientales de Colombia. 2021. Available on: <<https://www.minambiente.gov.co/index.php/sala-de-prensa/130-notas-de-interes/3998-la-conservacion-y-proteccion-del-suelo-es-otro-de-los-logros-ambientales-de-colombia>>. Accessed on: April. 2025.
- Minasny, B.; Tranter, G.; McBratney, A. B.; Brough, D. M.; Murphy, B. W. Regional transferability of mid-infrared diffuse reflectance spectroscopic prediction for soil chemical properties. *Geoderma*, v.153, p.155-162, 2009. <https://doi.org/10.1016/j.geoderma.2009.07.021>.
- Mukhamediev, R.; Merembayev, T.; Kuchin, Y.; Malakhov, D.; Zaitseva, E. Vitaly, L.; Popova, Y.; Symagulov, A.; Sagatdinova, G.; Amirgaliyev, Y. Soil salinity estimation for South Kazakhstan based on SAR Sentinel-1 and Landsat-8,9 OLI data with machine learning models. *Remote Sensing*. v.15, e4269, 2023. <https://doi.org/10.3390/rs15174269>
- Obando, E.; Carbonell, J. Caracterización espectral y mineralógica de los suelos del valle del río Cauca por espectroscopía visible e infrarroja. *Agronomía Colombiana*, v.28, p.291-301, 2010. <http://www.eolss.net/sample-chapters/c12/e1-05-07-01.pdf>
- Ordóñez, N.; Bolívar, A. Levantamiento agrológico del Centro Agropecuario. In: Universidad Nacional de Colombia; Instituto Geográfico Agustín Codazzi. Subdirección de Agrología. Bogotá: Imprenta Nacional de Colombia, 2014. 392p.
- Ortega-Monsalve, M.; Cerón-Muñoz, M. F.; Medina-Sierra, M. Espectroscopía de infrarrojo cercano para la determinación de materia orgánica y nitrógeno total del suelo. *Ciencia en Desarrollo*, v.14, p.111-118, 2023. <https://doi.org/10.19053/01217488.v14.n1.2023.1394>
- Piccini, C.; Metzger, K.; Debaene, G.; Stenberg, B.; Götzinger, S.; Borůvka, L.; Sandén, T.; Bragazza, L.; Liebisch, F. In-field soil spectroscopy in Vis-NIR range for fast and reliable soil analysis: A review. *European Journal of Soil Science*, v.75, e13481, 2024. <https://doi.org/10.1111/ejss.13481>
- Qadir, M.; Quillérou, E.; Nangia, V.; Murtaza, G.; Singh, M.; Thomas, R. J.; Drechsel, P.; Noble, A. D. Economics of salt-induced land degradation and restoration. *Natural Resources Forum*, v.38, p.282-295, 2014. <https://doi.org/10.1111/1477-8947.12054>
- Rincón, C. A.; Loaiza-Usuga, J. C.; Rubiano, Y.; Castañeda, D. Use of NIRS in soil properties evaluation related to soil salinity and sodicity in Colombian Caribbean coast. *Moscow University Soil Science Bulletin*, v.78, p.439-450, 2023. <https://doi.org/10.3103/S0147687423050046>
- Rodríguez-Pérez, J. R.; Marcelo, V.; Pereira-Obaya, D.; García-Fernández, M.; Sanz-Ablanedo, E. Estimating soil properties and nutrients by visible and infrared diffuse reflectance spectroscopy to characterize vineyards. *Agronomy*, v.11, e1895, 2021. <https://doi.org/10.3390/agronomy11101895>
- Saad, K.; Kallel, A.; Castaldi, F.; Sahli Chahed, T. Soil salinity detection and mapping by multi-temporal Landsat data: Zaghoun case study (Tunisia). *Remote Sensing*, v.16, e4761, 2024. <https://doi.org/10.3390/rs16244761>
- Soil Survey Staff. Keys to soil taxonomy. 13.ed. Lincoln: USDA - Natural Resources Conservation Service, 2022. 401p. Available at: <https://www.nrcs.usda.gov/resources/guides-and-instructions/keys-to-soiltaxonomy>. Accessed on: Sep. 2025.
- Tremblay, J. C.; Ainslie, P. N. Global and country-level estimates of human population at high altitude. *Proceedings of the National Academy of Sciences*, v.118, e2102463118, 2021. <https://doi.org/10.1073/pnas.2102463118>
- Tsolis, V.; Barouchas, P. Biochar as soil amendment: The effect of biochar on soil properties using VIS-NIR diffuse reflectance spectroscopy, biochar aging and soil microbiology—A review. *Land*, v.12, e1580, 2023. <https://doi.org/10.3390/land12081580>
- Viscarra, R. R. A.; Behrens, T.; Ben-Dor, E.; Chabrillat, S.; Dematté, J. A. L.; Ge, Y.; Gomez, C.; Guerrero, C.; Peng, Y.; Ramirez-Lopez, L.; Shi, Z.; Stenberg, B.; Webster, R.; Winowiecki, L.; Shen, Z. Diffuse reflectance spectroscopy for estimating soil properties: A technology for the 21st century. *European Journal of Soil Science*, v.73, e13271, 2022. <https://doi.org/10.1111/ejss.13271>
- Wang, J.; Zhen, J.; Hu, W.; Chen, S.; Lizaga, I.; Zeraatpisheh, M.; Yang, X. Remote sensing of soil degradation: Progress and perspective. *International Soil and Water Conservation Research*, v.11, p.429-454, 2023. <https://doi.org/10.1016/j.iswcr.2023.03.004>
- Webster, R.; Oliver, M.A. *Geostatistics for environmental scientists*. 1.ed. Hoboken, NJ: John Wiley & Sons Inc, 2007. 330p.